INSTITUTE OF PHYSICS PUBLISHING JOURNAL OF PHYSICS: CONDENSED MATTER

J. Phys.: Condens. Matter **15** (2003) 3539–3554 PII: S0953-8984(03)59249-9

Misfit dislocations in composites with nanowires

M Yu Gutkin, I A Ovid'ko and A G Sheinerman

Institute of Problems of Mechanical Engineering, Russian Academy of Sciences, Bolshoj 61, Vasil'yevskiy Ostrov, St Petersburg 199178, Russia

E-mail: ovidko@def.ipme.ru

Received 5 February 2003
Published 19 May 2003
Online at stacks.iop.org/JPhysCM/15/3539

Abstract

A theoretical model is suggested which describes the generation and evolution of misfit dislocations in composite solids containing nanowires with rectangular cross-section. In the framework of the model, the ranges of the geometric parameters (nanowire sizes, misfit parameter, interspacing between the nanowire and the free surface of the composite) are calculated at which the generation of various misfit dislocation configurations (loops, semi-loops and dipoles) is energetically favourable. Transformations of these dislocation configurations and their specific features are discussed.

1. Introduction

Composite solids exhibiting functional physical and mechanical properties serve as key materials in diverse contemporary high technologies. Recently, much attention has been attracted to nanocomposites which contain more than one solid phase and where at least one of the phases has dimensions less than 100 nanometres; see, e.g. [1–16]. In particular, of special interest for electronic and optoelectronic applications are nanocomposites containing nanowires (second-phase inclusions of wire form and cross-section having dimensions in the nanometre range) embedded into a matrix [1–11]. In addition to technologically motivated attention to nanowires, their examination is highly interesting for understanding the fundamental nature of nanoscale effects in condensed matter.

In general, the stability of both structure and properties of composite solids, which is crucial for applications of such solids, is strongly influenced by generation and evolution of misfit dislocations. Misfit dislocations are generated as defects that, in part, accommodate misfit stresses occurring due to a misfit (geometric mismatch) between adjacent crystalline lattices of different phases of a composite. Generation and evolution of misfit dislocations are crucially affected by geometric parameters of constituent phases of composites. The effect of the geometric parameters on behaviour of misfit dislocations is the subject of intensive experimental and theoretical studies which commonly deal with plate-like, continuous and island films deposited onto substrates, e.g., [17–36]. However, with the rapidly growing

 © 2003 IOP Publishing Ltd Printed in the UK

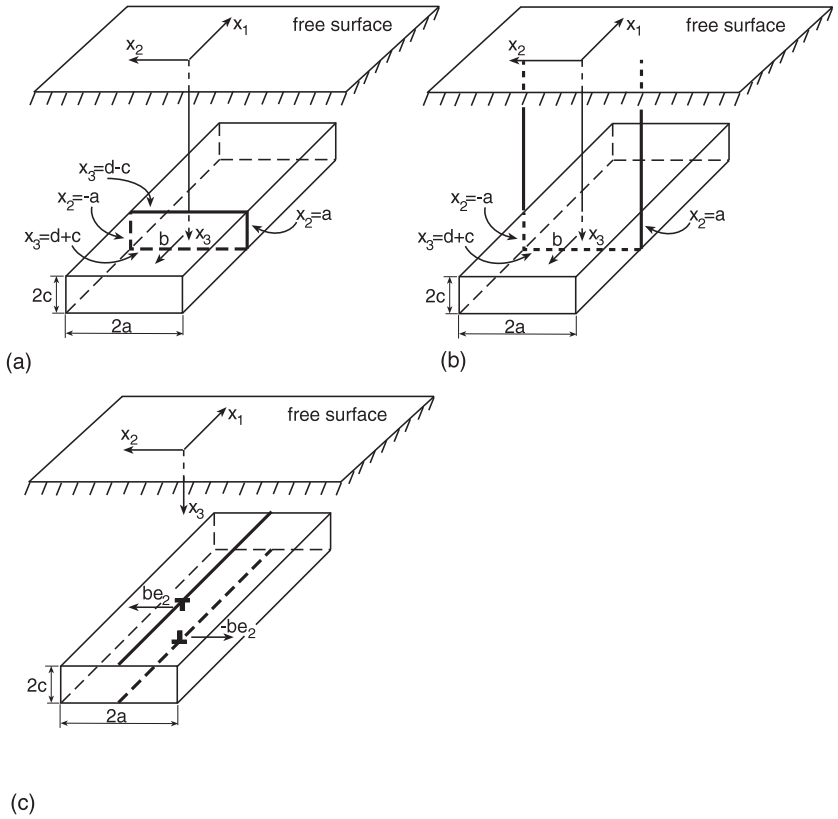

Figure 1. Misfit defect configurations in a composite containing a nanowire: (a) dislocation loop; (b) dislocation semi-loop, and (c) dislocation dipole.

attention to composites containing nanowires, it is highly interesting to analyse the behaviour of misfit dislocations in such composites. The aim of this paper is to elaborate a theoretical model which describes the influence of geometric parameters (misfit parameter, nanowire sizes, distance between nanowire and free surface) on the formation of various misfit dislocation configurations in composites containing nanowires with rectangular cross-sections.

2. Nanowire with a rectangular section in a composite

Let us consider a nanowire (a second-phase tube) having a rectangular cross-section and infinite length, embedded into a semi-infinite matrix (figure 1). The nanowire and matrix are assumed to be elastically isotropic solids with the same values of the shear modulus G and the same Poisson ratio ν. The nanowire is parallel to the matrix free surface, given by $x_3 = 0$, and is bounded by flat faces given by equations $x_2 = \pm a$ and $x_3 = d \pm c$. The interphase boundary between the matrix and the nanowire is characterized by a two-dimensional dilatation misfit $f = 2(a_m - a_i)/(a_m + a_i)$, where a_m and a_i are the crystal lattice parameters of crystal lattices of the matrix and the inclusion, respectively. Owing to the misfit f, elastic strains and stresses exist in both the inclusion and the matrix, which cause coherent matching of their adjacent crystal lattices. In general, these misfit stresses can be relaxed via the generation of various defect configurations, such as isolated misfit dislocations, misfit dislocation dipoles, prismatic

dislocation loops and semi-loops. Similar to misfit defects in conventional continuous films and film islands (see, e.g., [17–36]), the formation of misfit defect configurations in nanowires is energetically favourable in certain ranges of parameters of the composite system under consideration.

First, let us consider conditions at which the formation of a prismatic dislocation loop at the interphase boundary between the nanowire and the matrix is energetically favourable. Such a loop can result from either preliminary generation of dislocation semi-loops at the matrix free surface or coagulation of point defects (interstitials or vacancies). Let the prismatic dislocation loop be located in the plane $x_1 = 0$ and bounded by the segments $x_2 = \pm a$ and $x_3 = d \pm c$ (figure 1(a)). It is characterized by the Burgers vector $\boldsymbol{b} = -b\boldsymbol{e}_1$. The formation of the prismatic dislocation loop is energetically favourable if the difference ΔW in the energy between the dislocated state and the dislocation-free state of the composite is negative ($\Delta W < 0$) [18]. The characteristic energy difference can be written as follows:

$$\Delta W = W^l + W^{l-f} + W^c. \tag{1}$$

Here W^l denotes the proper strain energy of the dislocation loop, W^{l-f} the energy that characterizes the elastic interaction between the dislocation and the misfit stresses, and W^c the dislocation core energy.

3. Energy of a prismatic dislocation loop located near a free surface

In order to calculate the proper strain energy W^l of a prismatic dislocation loop, first, it is necessary to calculate its stress field in the region surrounded by the loop. To date, the elastic fields have been calculated for dislocation loops having the form of a circle [37–50], rectangle [51–54] and ellipse [55–57] in isotropic [37–43, 51, 52] and anisotropic [56, 57] infinite media as well as in isotropic semi-infinite solids [38, 44, 45], two-phase composite materials [46–48], isotropic [49] and anisotropic [50] plates in the case of loops located in planes parallel to a free surface or an interphase boundary. At the same time, the authors are unaware of similar solutions for prismatic loops whose planes are perpendicular to a free surface.

Elastic fields of the loop under consideration (figure 1), which is located in the plane perpendicular to the matrix free surface, will be calculated below with the help of the Green functions for semi-infinite solids [58, 59]. (Generally speaking, displacements created by the dislocation loop can be calculated using the general formulas [60–63] for displacement fields of infinitesimal dislocation loops in semi-infinite isotropic solids. However, the use of the Green functions is more effective, because the displacement fields [60–63] are not expressed in the direct way.)

The displacement field u_i created by a prismatic dislocation loop can be written as follows [59]:

$$u_i(\boldsymbol{x}) = \int_\Omega C_{jlmn}\beta^*_{nm}(\boldsymbol{x}')\frac{\partial}{\partial x'_l}G_{ij}(\boldsymbol{x}, \boldsymbol{x}')\,\mathrm{d}\boldsymbol{x}', \tag{2}$$

where $\boldsymbol{x} = (x_1, x_2, x_3)$ and $\boldsymbol{x}' = (x'_1, x'_2, x'_3)$ are three-dimensional vectors, $\mathrm{d}\boldsymbol{x}' = \mathrm{d}x'_1\,\mathrm{d}x'_2\,\mathrm{d}x'_3$, Ω is the half-space $x_3 \geqslant 0$, $\beta^*_{nm}(\boldsymbol{x}')$ is the plastic distortion created by the dislocation loop, C_{jlmn} denotes the tensor of elastic moduli, and $G_{ij}(\boldsymbol{x}, \boldsymbol{x}')$ is the Green function for a half-space. In formula (2) and below, summation is performed over repeated indexes. In the case of isotropic solids, the tensor C_{jlmn} reads [59]:

$$C_{jlmn} = \lambda\delta_{jl}\delta_{mn} + G(\delta_{jn}\delta_{lm} + \delta_{jm}\delta_{ln}), \tag{3}$$

where $\lambda = 2\nu G/(1 - 2\nu)$, and δ_{mn} is the Kronecker symbol.

The plastic distortion β^*_{nm} created by the dislocation loop (figure 1(a)) is as follows:

$$\beta^*_{nm}(\boldsymbol{x}') = b\delta(x'_1)H(a-|x'_2|)H(c-|x'_3-d|)\delta_{n1}\delta_{m1}. \tag{4}$$

Here $\delta(t)$ is the delta-function, and $H(t)$ is the Heaviside function ($H(t)=1$, if $t>0$, and 0, if $t<0$).

Formulas for the Green functions G_{kl} are given (in units of $1/[16\pi G(1-\nu)]$) by [59]:

$$G_{ij}(\boldsymbol{x},\boldsymbol{x}') = G_{ji}(\boldsymbol{x},\boldsymbol{x}') = \left\{\frac{3-4\nu}{R_1}+\frac{4(1-\nu)(1-2\nu)}{R_2+x_3+x'_3}+\frac{R_2^2+2x_3x'_3}{R_2^3}\right\}\delta_{ij} + (x_i-x'_i)(x_j-x'_j)\left\{\frac{1}{R_1^3}-\frac{4(1-\nu)(1-2\nu)}{R_2(R_2+x_3+x'_3)^2}+\frac{(3-4\nu)R_2^2-6x_3x'_3}{R_2^5}\right\}, \tag{5}$$

$$G_{3j}(\boldsymbol{x},\boldsymbol{x}') = (x_j-x'_j)\left\{(x_3-x'_3)\left[\frac{1}{R_1^3}+\frac{3-4\nu}{R_2^3}\right]+\frac{4(1-\nu)(1-2\nu)}{R_2(R_2+x_3+x'_3)}-\frac{6x_3x'_3(x_3+x'_3)}{R_2^5}\right\}, \tag{6}$$

$$G_{i3}(\boldsymbol{x},\boldsymbol{x}') = (x_i-x'_i)\left\{(x_3-x'_3)\left[\frac{1}{R_1^3}+\frac{3-4\nu}{R_2^3}\right]-\frac{4(1-\nu)(1-2\nu)}{R_2(R_2+x_3+x'_3)}+\frac{6x_3x'_3(x_3+x'_3)}{R_2^5}\right\}, \tag{7}$$

$$G_{33}(\boldsymbol{x},\boldsymbol{x}') = \frac{3-4\nu}{R_1}+\frac{(x_3-x'_3)^2}{R_1^3}+\frac{8(1-\nu)^2-(3-4\nu)}{R_2} + \frac{(3-4\nu)(x_3+x'_3)^2-2x_3x'_3}{R_2^3}+\frac{6x_3x'_3(x_3+x'_3)^2}{R_2^5}, \tag{8}$$

where $i,j=1,2$, and $R^2_{1,2}=(x_1-x'_1)^2+(x_2-x'_2)^2+(x_3\mp x'_3)^2$.

With (3) and (4) substituted to (2), we have:

$$u_i(\boldsymbol{x}) = \frac{2Gb}{1-2\nu}\int_{d-c}^{d+c}\mathrm{d}x'_3\int_{-a}^{a}\mathrm{d}x'_2\left\{(1-\nu)\frac{\partial G_{i1}}{\partial x'_1}+\nu\left(\frac{\partial G_{i2}}{\partial x'_2}+\frac{\partial G_{i3}}{\partial x'_3}\right)\right\}\Bigg|_{x'_1=0}. \tag{9}$$

The elastic distortion β_{ji} created by the dislocation loop is in the following relationship with the displacement vector u_i:

$$\beta_{ji}(\boldsymbol{x}) = \frac{\partial u_i(\boldsymbol{x})}{\partial x_j}-\beta^*_{ji}(\boldsymbol{x}). \tag{10}$$

The stress field σ^l_{ij} of the dislocation loop is given by [59]:

$$\sigma^l_{ij}(\boldsymbol{x}) = C_{ijkl}\beta_{lk}(\boldsymbol{x}). \tag{11}$$

The elastic energy of the dislocation loop is calculated using formula [39, 59]:

$$W^l = -\frac{b}{2}\int_{d-c+r_0}^{d+c-r_0}\mathrm{d}x_3\int_{-a+r_0}^{a-r_0}\mathrm{d}x_2\,\sigma^l_{11}(x_1=0) \tag{12}$$

with r_0 being the dislocation core radius.

With (3) and (9)–(11) substituted to (12) and conditions $G_{12}=G_{21}$, $\frac{\partial G_{kl}}{\partial x'_1}=-\frac{\partial G_{kl}}{\partial x_1}$, $\frac{\partial G_{kl}}{\partial x'_2}=-\frac{\partial G_{kl}}{\partial x_2}$, $(k,l=1,2,3)$, $\frac{\partial G_{13}}{\partial x'_3}=-\frac{\partial G_{31}}{\partial x_3}$ and $\frac{\partial G_{23}}{\partial x'_3}=-\frac{\partial G_{32}}{\partial x_3}$ taken into account, we obtain the following expression for the energy W^l:

$$W^l = -\frac{2G^2b^2}{(1-2\nu)^2}\int_{d-c+r_0}^{d+c-r_0}\mathrm{d}x_3\int_{-a+r_0}^{a-r_0}\mathrm{d}x_2\left\{\int_{d-c}^{d+c}\mathrm{d}x'_3\int_{-a}^{a}\mathrm{d}x'_2\left[(1-\nu)^2\frac{\partial^2 G_{11}}{\partial x_1\partial x'_1} + 2\nu(1-\nu)\left(\frac{\partial^2 G_{21}}{\partial x_2\partial x'_1}+\frac{\partial^2 G_{31}}{\partial x_3\partial x'_1}\right)+\nu^2\left(\frac{\partial^2 G_{22}}{\partial x_2\partial x'_2}+2\frac{\partial^2 G_{32}}{\partial x_3\partial x'_2}+\frac{\partial^2 G_{33}}{\partial x_3\partial x'_3}\right)\right]\Bigg|_{x'_1=0} - \frac{(1-\nu)(1-2\nu)}{2}\delta(x_1)\right\}\Bigg|_{x_1=0}. \tag{13}$$

After integration in formula (13) under the condition $(d, c) \gg r_0/2$, we have $W^l = (Db^2/2)L_1$, where $D = G/[2\pi(1-\nu)]$ and the effective length $L_1 = L_1(a, c, d, \nu, r_0)$ reads

$$L_1(a,c,d,\nu,r_0) = S_1 + 2S_2 + S_3 + [3-4\nu(3-2\nu)]S_4 + 2\frac{1-2\nu(6-11\nu+8\nu^3)}{(1-2\nu)^2}S_5 - \frac{129-2\nu\{234-\nu[245-4\nu(5+16\nu)]\}}{3(1-2\nu)^2}S_6, \tag{14}$$

with

$$S_1 = a\left(2\ln\frac{K_3+a}{K_3-a} - \ln\frac{\sqrt{a^2+(d-c+r_0/2)^2}+a}{\sqrt{a^2+(d-c+r_0/2)^2}-a} - \ln\frac{K_2+a}{K_2-a}\right), \tag{15}$$

$$S_2 = 2a\ln\frac{4a}{r_0} + 2c\ln\frac{4c}{r_0} - a\ln\frac{K_4+a}{K_4-a} - c\ln\frac{K_4+c}{K_4-c} - 4(a+c-K_4), \tag{16}$$

$$S_3 = \frac{8(1-\nu)(1-2\nu)c^2d}{a^2} + \frac{3c^2}{d} - \frac{2c^2(a^2+d^2)K_3}{a^2d^2}, \tag{17}$$

$$S_4 = \frac{2d^2K_3 - (d-c)^2K_1 - (d+c)^2K_2}{2a^2}, \tag{18}$$

$$S_5 = d\ln\frac{d+K_3}{d} - (d-c)\ln\frac{d-c+K_1}{d-c} - (d+c)\ln\frac{d+c+K_2}{d+c}, \tag{19}$$

$$S_6 = 2K_3 - K_1 - K_2, \tag{20}$$

and $K_{1,2}^2 = a^2 + (d \mp c)^2$, $K_3^2 = a^2 + d^2$, $K_4^2 = a^2 + c^2$.

In the limit $d \to \infty$, the expression for the energy W^l transforms into that for the energy W_∞^l of a prismatic dislocation loop in an infinite medium:

$$W_\infty^l = 2Db^2\left\{a\ln\frac{4a}{r_0} + c\ln\frac{4c}{r_0} - \frac{a}{2}\ln\frac{K_4+a}{K_4-a} - \frac{c}{2}\ln\frac{K_4+c}{K_4-c} - 2(a+c-K_4)\right\}. \tag{21}$$

For a square loop, at $2a = 2c = l$ (l is the length of a segment), expression (21) yields the energy density $W_\infty^l/(4l) \approx Db^2/2\,(\ln l/r_0 - 0.78)$ per unit loop length, which is in good agreement with similar results for a prismatic loop of hexagonal shape ($\approx Db^2/2\,(\ln l/r_0 + 0.16)$ and $\approx Db^2/2\,(\ln l/r_0 - 0.14)$, where l is the length of a segment of a hexagonal loop), discussed in [64].

In the limit $a \to \infty$, the elastic energy of the dislocation loop, divided by $2a$, transforms into the elastic energy (per unit length) $w_\parallel^{dip}$ of a dipole of edge dislocations which are parallel to the matrix free surface:

$$w_\parallel^{dip} = \lim_{a\to\infty}\frac{W^l}{2a} = \frac{Db^2}{2}\left(\ln\frac{d-c+r_0/2}{r_0/2} + \ln\frac{d+c}{r_0/2} - 2\ln\frac{d}{c} - \frac{c^2}{d^2}\right). \tag{22}$$

For $c \to \infty$, the elastic energy of the dislocation loop (divided by $2c$) is equal to the elastic energy $w_\perp^{dip}$ of a dipole of edge dislocations (per their unit length) whose lines are perpendicular to the free surface:

$$w_\perp^{dip} = \lim_{c\to\infty}\frac{W^l}{2c} = \frac{Db^2}{2}\ln\frac{2a}{r_0}. \tag{23}$$

This formula coincides with that for elastic energy of a similar dislocation dipole in an infinite medium [64]. Finally, the elastic energy W^{sl} of a Π-like dislocation semi-loop can be found from formulas (14)–(20) in the limit of $d \to c$: $W^{sl} = \lim_{d\to c} W^l$.

We can also give here a useful first-order approximation to the energy W_{lat}^{segm}, related to the formation of a lateral segment perpendicular to the free surface. It is defined as the

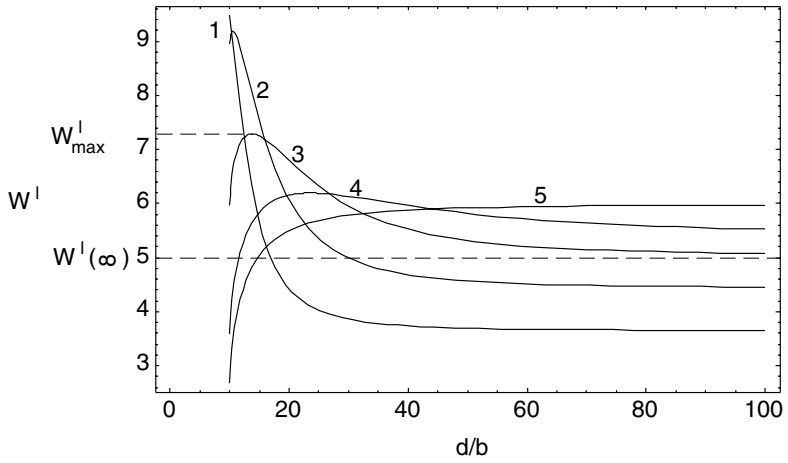

Figure 2. Dependence of the proper energy W^l (in units of $Db^3/[4(a+c)]$) of the misfit dislocation loop on the dimensionless interspacing d/b between its centre line and the matrix free surface, for $\nu = 0.3$, $r_0 = b$, $c/b = 10$ and $a/b = 5$, 10, 20, 40 and ∞ (curves 1, 2, 3, 4 and 5, respectively). Dashed lines correspond to values of W^l_{max} and $W^l(\infty)$ for curve 3.

half-difference of the elastic energy W^{sl} of the dislocation semi-loop and the elastic energy of its straight segment of length $2a$, parallel to the free surface, at $a \to \infty$:

$$W^{segm}_{lat} = \tfrac{1}{2} \lim_{a\to\infty} [W^{sl} - 2a w^{dip}_{\parallel}(d = c)]$$
$$= \frac{Db^2c}{4}\left(\ln\frac{4c}{r_0} + \frac{[1 - 2\nu(6 - 11\nu + 8\nu^3)]\ln 2}{(1-2\nu)^2} - \frac{1}{4}\right). \tag{24}$$

The total energy related to the formation of a lateral segment is a combination of its elastic energy W^{segm}_{lat} and the energy Db^2c of its core.

Dependences of the energy W^l on the interspacing d between the centre of the dislocation loop and the matrix free surface are shown in figure 2, for $c = 10b$, $r_0 = b$, $\nu = 0.3$ and different values of a. As follows from figure 2, the energy W^l decreases with rising d at low values of a/c (for example, see curve 1 with $a = c/2$). When the ratio a/c increases, the dependence $W^l(d)$ exhibits a maximum $W^l = W^l_{max}$ at some d (see curve 2 with $a = c$). At high values of a/c, the height $W^l_{max} - W^l_\infty$, where $W^l_\infty = W^l(d \to \infty)$, of the maximum decreases (see curves 3 and 4 with $a = 2c$ and $4c$, respectively) and approaches zero in the limit of $a \to \infty$ (see curve 5).

4. Interaction of a dislocation loop with misfit stress field

The energy W^{l-f} that characterizes interaction of the dislocation loop (figure 1(a)) with the misfit stress field is calculated using the formula [39]:

$$W^{l-f} = -b\int_{d-c}^{d+c} \mathrm{d}x_3 \int_{-a}^{a} \mathrm{d}x_2\, \sigma^f_{11}(x_1 = 0). \tag{25}$$

Here σ^f_{11} is the component of the stress tensor of the second-phase nanowire.

The stresses σ^f_{kl} are calculated using the expressions for the stresses created by a rectangular inclusion in a plate of finite thickness [65]. In units of $2D(1+\nu)f$, they are as follows:

$$\sigma^f_{11} = \sigma^f_{22} + \sigma^f_{33}, \tag{26}$$

$$\sigma_{22}^f = \arctan\frac{a-x_2}{d+c-x_3} + \arctan\frac{a+x_2}{d+c-x_3} - \arctan\frac{a-x_2}{d-c-x_3} - \arctan\frac{a+x_2}{d-c-x_3}$$
$$- 3\,\mathrm{arccotan}\frac{(d-c+x_3)^2+x_2^2-a^2}{2a(d-c+x_3)} + 3\,\mathrm{arccotan}\frac{(d+c+x_3)^2+x_2^2-a^2}{2a(d+c+x_3)}$$
$$+ \frac{4ax_3[(d-c+x_3)^2-x_2^2+a^2]}{[(d-c+x_3)^2+(a-x_2)^2]\,[(d-c+x_3)^2+(a+x_2)^2]}$$
$$- \frac{4ax_3[(d+c+x_3)^2-x_2^2+a^2]}{[(d+c+x_3)^2+(a-x_2)^2]\,[(d+c+x_3)^2+(a+x_2)^2]}, \tag{27}$$

$$\sigma_{33}^f = \arctan\frac{d+c-x_3}{a-x_2} + \arctan\frac{d+c-x_3}{a+x_2} - \arctan\frac{d-c-x_3}{a-x_2} - \arctan\frac{d-c-x_3}{a+x_2}$$
$$- \mathrm{arccotan}\frac{(d-c+x_3)^2+x_2^2-a^2}{2a(d-c+x_3)} + \mathrm{arccotan}\frac{(d+c+x_3)^2+x_2^2-a^2}{2a(d+c+x_3)}$$
$$- \frac{4ax_3\,[(d-c+x_3)^2-x_2^2+a^2]}{[(d-c+x_3)^2+(a-x_2)^2]\,[(d-c+x_3)^2+(a+x_2)^2]}$$
$$+ \frac{4ax_3\,[(d+c+x_3)^2-x_2^2+a^2]}{[(d+c+x_3)^2+(a-x_2)^2]\,[(d+c+x_3)^2+(a+x_2)^2]}, \tag{28}$$

$$\sigma_{12}^f = \sigma_{13}^f = 0, \tag{29}$$

$$\sigma_{23}^f = \frac{1}{2}\ln\frac{[(d+c-x_3)^2+(a+x_2)^2]\,[(d-c-x_3)^2+(a-x_2)^2]}{[(d+c-x_3)^2+(a-x_2)^2]\,[(d-c-x_3)^2+(a+x_2)^2]}$$
$$+ \frac{1}{2}\ln\frac{[(d-c+x_3)^2+(a+x_2)^2]\,[(d+c+x_3)^2+(a-x_2)^2]}{[(d-c+x_3)^2+(a-x_2)^2]\,[(d+c+x_3)^2+(a+x_2)^2]}$$
$$- \frac{8ax_2x_3\,(d-c+x_3)}{[(d-c+x_3)^2+(a-x_2)^2]\,[(d-c+x_3)^2+(a+x_2)^2]}$$
$$+ \frac{8ax_2x_3\,(d+c+x_3)}{[(d+c+x_3)^2+(a-x_2)^2]\,[(d+c+x_3)^2+(a+x_2)^2]}. \tag{30}$$

Substituting (26)–(28) into (25), one obtains $W^{l-f} = -(Db^2/2)\,f\,L_2$, where the effective length $L_2 = L_2(a, c, d)$ is given for $d > c$ by

$$L_2(a,c,d) = 128(1+\nu)\frac{a}{b}\left\{\frac{\pi c}{4} + 2d\arctan\frac{d}{a} - (d-c)\arctan\frac{d-c}{a} - (d+c)\arctan\frac{d+c}{a}\right.$$
$$\left. + \frac{d^2}{2a}\ln\frac{d^2-c^2}{d^2} + \frac{d^2-a^2}{2a}\ln\frac{K_3^2}{K_1K_2} + \frac{dc}{a}\ln\frac{(d+c)K_1}{(d-c)K_2} - \frac{c^2}{2a}\ln\frac{K_1K_2}{d^2-c^2}\right\}. \tag{31}$$

5. Critical condition of the energetically favourable formation of a misfit dislocation loop

The formation of a dislocation loop is energetically favourable, if $\Delta W < 0$. With formula (1) and equations $W^l = (Db^2/2)L_1$, $W^{l-f} = -(Db^2/2)\,f\,L_2$ and $W^c \approx (Db^2/2)L$ (the energy W^c of dislocation loop core is given by this standard approximation [64], where $L = 4(a+c)$ is the sum length of dislocation segments composing the loop), the inequality $\Delta W < 0$ is equivalent to the condition $f > f_c^l$ with

$$f_c^l = \frac{L+L_1}{L_2}, \tag{32}$$

where L_1 is determined by equations (14)–(20) and L_2 is given by equation (31).

In doing so, f_c^l plays the role of the critical misfit parameter. When the misfit parameter f that characterizes the nanowire material exceeds f_c^l, the formation of such a prismatic dislocation loop (figure 1(a)) is energetically favourable.

6. Misfit dislocation semi-loops in composites with nanowires

Besides the formation of prismatic dislocation loops surrounding a nanowire, alternative mechanisms can come into play, also causing a partial relaxation of misfit stresses. These mechanisms are related to the formation of either misfit dislocation semi-loops (figure 1(b)) or misfit dislocation dipoles (figure 1(c)).

In this section, we consider energetic characteristics of Π-like semi-loops of misfit dislocations (figure 1(b)). In the case of a wide nanowire located in the vicinity of the matrix free surface, the total length of such a semi-loop (and, as a corollary, the energy of its core) is small compared to that of a dislocation loop surrounding the nanowire. Therefore, the formation of misfit dislocation semi-loops can be more energetically favourable than the generation of closed dislocation loops. Also, the critical misfit parameter f_c^{sl} for the formation of semi-loops may be smaller than the critical misfit parameter f_c^l for the generation of dislocation loops ($f_c^{sl} < f_c^l$). In doing so, the critical misfit parameter f_c^{sl} is defined as follows: if $f > f_c^{sl}$, the formation of an individual misfit dislocation semi-loop is energetically favourable.

The critical misfit parameter f_c^{sl} is calculated in the same way as f_c^l (see above). So, we have calculated dependences of f_c^l and f_c^{sl} on the distance h between the nanowire and the matrix free surface ($h = d - c$). These dependences are presented in figure 3 for different values of a in the case of $c = 3b$ (figure 3(a)) and for different values of c in the case of $a = 15b$ (figure 3(b)). As follows from figure 3(a), the character of the curves $f_c^l(h)$ (solid curves) is close to that of curves $W^l(d)$ shown in figure 2. That is, f_c^l monotonically decreases with rising h at low a/c (see curve 1 with $a = c$ in figure 3(a)), and has a maximum in the case of the intermediate values of a/c (see curves 2, 3 and 4 with $a/c = 3$, 8 and 15, respectively, in figure 3(a)). The maximum disappears in the limit of $a \to \infty$ (see curve 5 in figure 3(a)) corresponding to the transformation of a nanowire into a plate-like inclusion and the conversion of a dislocation loop into a dislocation dipole. The critical misfit parameter f_c^{sl} for the energetically favourable formation of dislocation semi-loops is either lower than f_c^l at low h (see curves 1 and 1′ in figure 3(b)) or larger than f_c^l at any $h \geqslant b$ (see curves 3 and 3′ in figure 3(b)).

When the interspacing h between the nanowire and the matrix free surface increases, either the defect-free state or the formation of misfit dislocation loops becomes energetically favourable. The interspacing h may increase during the growth of the composite, say, by deposition of new atomic layers on its free surface. In doing so, in particular, the following consequent transformation of the interphase boundary state can occur with rising h: the state with a dislocation semi-loop (figure 1(b)) transforms into the defect-free state which then transforms into the state with a misfit dislocation loop (figure 1(a)). For an illustration of this transformation, dependences $f_c^l(h)$ and $f_c^{sl}(h)$ are presented in figure 3(c), which correspond to curves 3 and 3′ in figure 3(a), respectively. These curves separate the regions α where the formation of dislocation loops is energetically favourable, the regions β where the formation of dislocation semi-loops is energetically favourable, the regions γ where the formation of both dislocation loops and semi-loops is preferred compared to the defect-free state, and the regions δ where the defect-free state is energetically favourable. In the case presented in figure 3(c), both dislocation loops and semi-loops are unfavourable at low values of the misfit parameter f (say, $f = 0.02$) and any values of h. At intermediate values of f (say, $f = 0.028$) dislocation semi-loops are preferred in the range of low h. However, they become unfavourable with

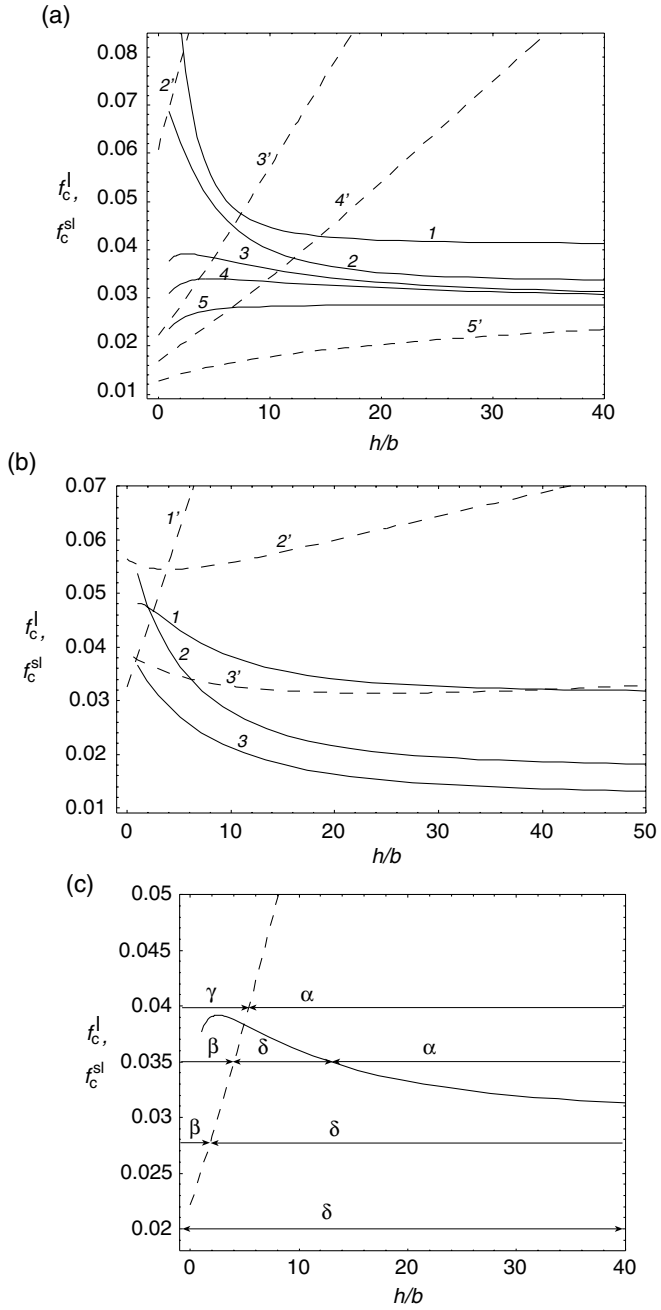

Figure 3. Dependences of critical misfit parameters f_c^l (solid curves) and f_c^{sl} (dashed curves) on the dimensionless interspacing h/b between the nanowire and the matrix free surface, for $\nu = 0.3$, $r_0 = b$, and (a) $c/b = 3$, while $a/b = 3$ (curve 1), 9 (curves 2 and 2′), 24 (curves 3 and 3′), 45 (curves 4 and 4′), and ∞ (curves 5 and 5′); (b) $a/b = 15$, while $c/b = 3$ (curves 1 and 1′), 10 (curves 2 and 2′), 30 (curves 3 and 3′); (c) $c/b = 3$ and $a/b = 24$. Curve 1′ is not shown in (a), because it corresponds to the range of very large values of the misfit parameter ($f > 0.1$). Horizontal lines in figure 3(c) show values of the misfit parameter f. Greek letters α, β, γ and δ denote the parameter regions where different (defected and non-defected) states of the system are energetically favourable: α—loops, β—semi-loops, γ—both loops and semi-loops, and δ—non-defected state.

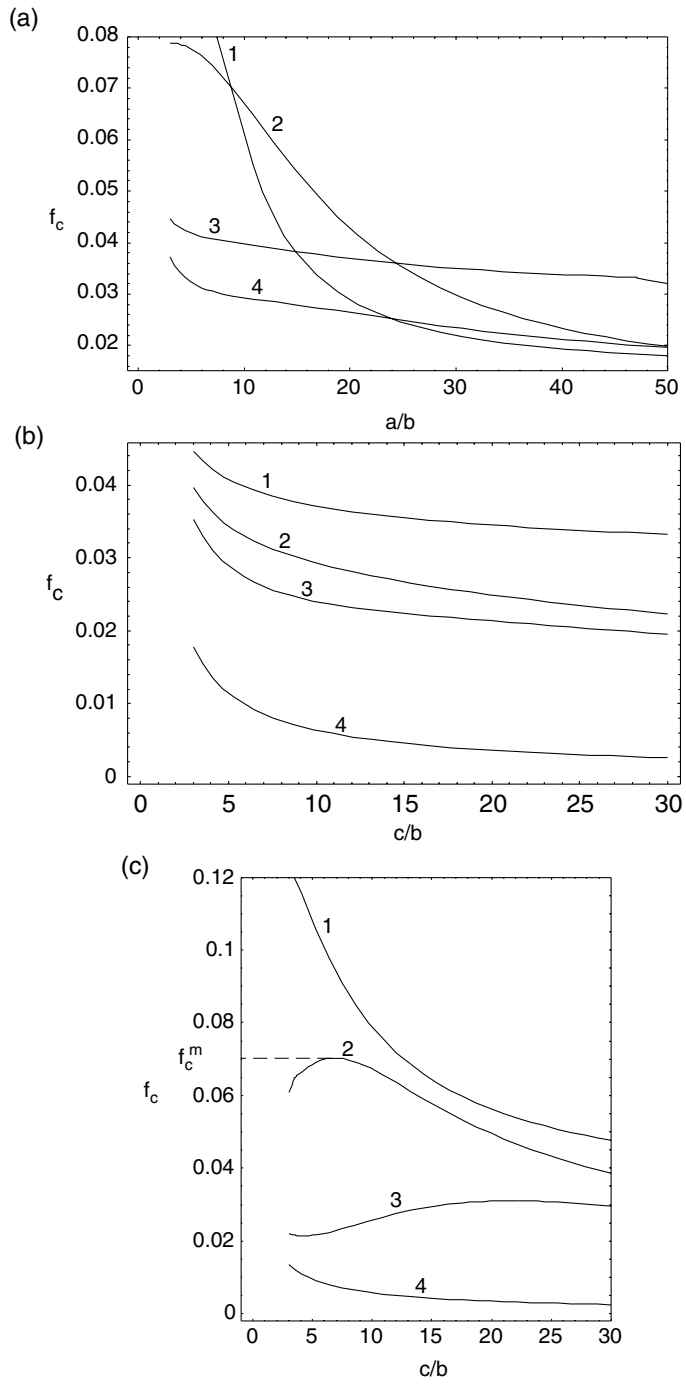

Figure 4. Critical misfit parameter f_c as a function of the dimensionless (a) semi-width a/b, and (b), (c) semi-height c/b of a nanowire, for $r_0 = b$, $\nu = 0.3$ and the following values of parameters: (a) $h = b$, $c = 3b$ (curve 1), $h = b$, $c = 10b$ (curve 2), $h = 10b$, $c = 3b$ (curve 3), and $h = 10b$, $c = 10b$ (curve 4); (b) $h = 10b$, while $a/b = 3$, 10, 30, and ∞ (curves 1, 2, 3, and 4, respectively); (c) $h = b$, while $a/b = 3$, 10, 30 and ∞ (curves 1, 2, 3 and 4, respectively).

rising h. At large values of f (say, $f = 0.035$) the energetically preferred state changes with rising h as follows: dislocation semi-loops (phase region β) $\rightarrow$ the defect-free state (phase region δ) $\rightarrow$ dislocation loops (phase region α). When horizontal line corresponding to the misfit parameter f is located above the point where curves f_c^l and f_c^{sl} intersect (say, at $f = 0.04$), both dislocation loops and semi-loops are preferred at low h, and the latter transform into dislocation loops with rising h.

In figure 4, the dependences of the critical misfit parameter $f_c = \min\{f_c^l,\ f_c^{sl}\}$ (which characterizes the energetically favourable formation of either dislocation loops or semi-loops) on nanowire sizes a and c are shown. As follows from figure 4(a), f_c monotonically decreases with increasing the nanowire semi-width a. When the nanowire is highly distant from the matrix free surface, f_c decreases with increasing c (figure 4(b)), similar to the critical misfit parameter for the formation of misfit dislocation dipoles in capped films [66, 67], which is equal to f_c in the limit of $a \rightarrow \infty$. However, when the nanowire is closely distant from the matrix free surface, the dependence $f_c(c)$ has a more complicated character (figure 4(c)). So, f_c decreases with increasing c at low values of a (see curve 1 in figure 4(c)). The curve $f_c(c)$ has a maximum $f_c = f_c^m$ at intermediate values of a (see curve 2 in figure 4(c)). In the situation discussed, if $f > f_c$, the formation of either dislocation loops or semi-loops (which occurs as an energetically favourable process at $f > f_c$) is realized at any value of the nanowire semi-height c. For large values of a, the dependence $f_c(c)$ has two extrema, maximum and minimum (see curve 3 in figure 4(c)). In the limit of $a \rightarrow \infty$, f_c monotonically decreases with increasing c (see curve 4 in figure 4(c)). As follows from figure 4(a) and (b), in the case where the nanowire is highly distant from the matrix free surface, misfit dislocation loops and semi-loops are formed in the composite with a given value of f if the nanowire sizes a and c exceed their critical values. In particular, misfit dislocation loops or semi-loops are energetically favourable in the composite with a given value of c if $f > f_c(a \rightarrow \infty)$ and a exceeds some critical value (figure 4(a)). If $f < f_c(a \rightarrow \infty)$, misfit dislocation configurations are unfavourable at any value of a. Also, misfit dislocation configurations in the composite with a given value of a are favourable at large c, if $f > f_c(c \rightarrow \infty)$, and always unfavourable, if $f < f_c(c \rightarrow \infty)$ (see figure 4(c)).

When the interspacing h between the nanowire and the matrix free surface is small, in some cases misfit dislocation loops or semi-loops are formed if the nanowire has a large enough thickness (curves 1 and 4 in figure 4(c)), while in other cases they are generated only if the nanowire thickness is not too large (see curve 3 in figure 4(c)).

In figure 5, the lines of constant levels of the critical misfit f_c in the coordinate space $(a/b,\ c/b)$ are presented for different values of h. The maps illustrate that if the distance h is very small, the dependences f_c on c have maximums (figure 5(a)), which are absent if h is sufficiently large (figures 5(b), (c)). From figure 5 it also follows that if the nanowire is far enough from the free surface, for small a and large c, f_c depends primarily on a and very weakly depends on c, while for small c and large a, f_c depends primarily on c. That means that in this case, the value of f_c is governed by the size of its smallest side.

7. Misfit dislocation dipoles in composites with nanowires

In general, together with misfit dislocation loops (figure 1(a)) and semi-loops (figure 1(b)), dipoles of misfit dislocations formed at the interphase boundary between the nanowire and the matrix (figure 1(c)) are capable of effectively contributing to relaxation of misfit stresses. As with dislocation loops and semi-loops, the formation of misfit dislocation dipoles is energetically favourable if the misfit parameter f exceeds the corresponding critical value f_c^{dip}. This critical misfit parameter f_c^{dip} for dislocation dipole formation is calculated in

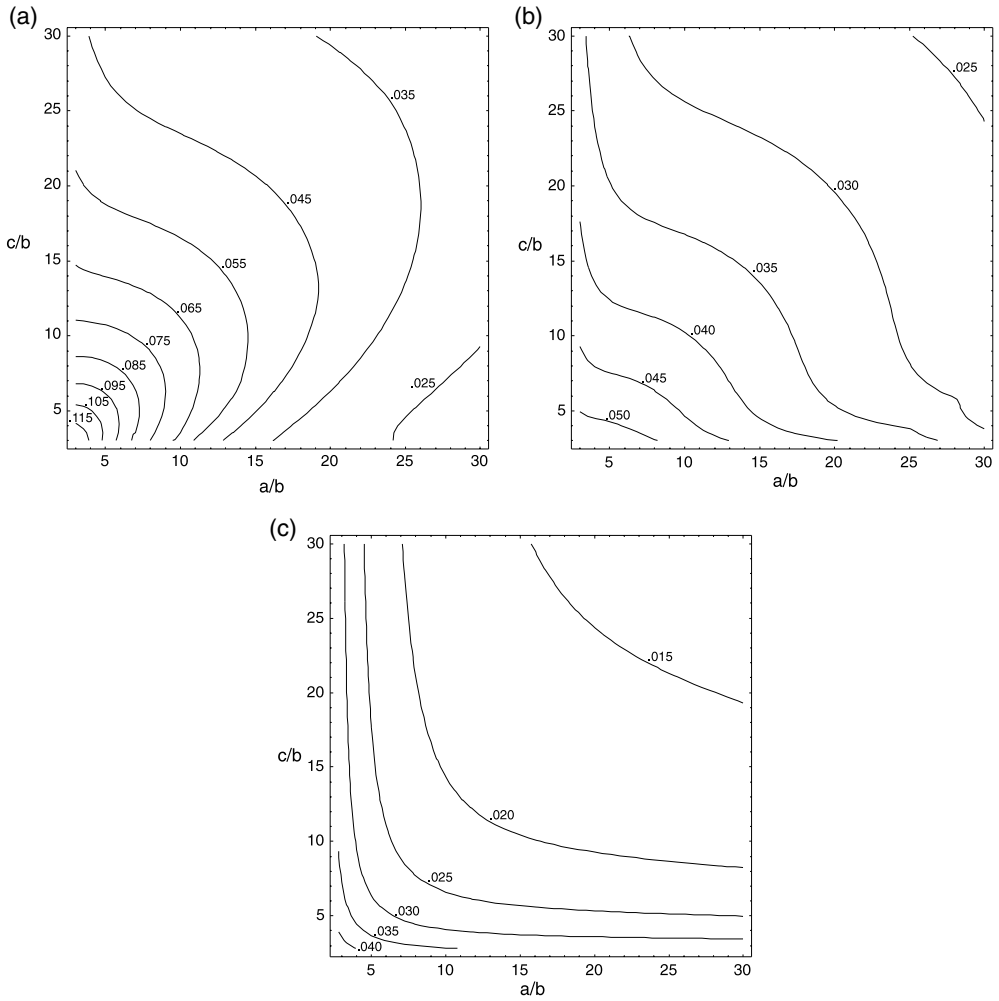

Figure 5. The maps of the critical misfit f_c in the coordinate space $(a/b, c/b)$ for $\nu = 0.3$, $r_0 = b$; $h/b = 1$ (a), 5 (b) and 25 (c).

the same way as the critical misfit parameter f_c^l for dislocation loop formation (see above). In doing so, we have calculated the dependences of f_c^{dip} on h (see figure 6), for values of parameters used in calculation of curves $f_c^l(h)$ and $f_c^{sl}(h)$ presented in figure 3(a). As follows from figure 6, f_c^{dip} decreases with increasing the nanowire semi-width a. At low a, the critical misfit parameter f_c^{dip} increases with increasing h (see curve 1 in figure 6). At intermediate values of a the function $f_c^{dip}(h)$ has a minimum (curve 2 in figure 6). With further increase of a, the function $f_c^{dip}(h)$ firstly increases and then decreases (see curves 3 and 4 in figure 6). In the limit of $a \to \infty$, $f_c^{dip}(h)$ monotonically increases with increasing h.

The dependences of f_c^{dip} on the nanowire semi-height c and the maps of f_c^{dip} in the coordinate space $(a/b, c/b)$ are shown in figures 7(a) and (b), for values of parameters used in the calculation of the curves presented in figures 4(c) and 5(a), respectively. As follows from figure 7, f_c^{dip} decreases with increasing one of the nanowire sizes, a or c, even in the situation where the nanowire is close to the matrix free surface (h is small). That is, in contrast to the case of dislocation loops and semi-loops (see above), the effect of the free surface on the

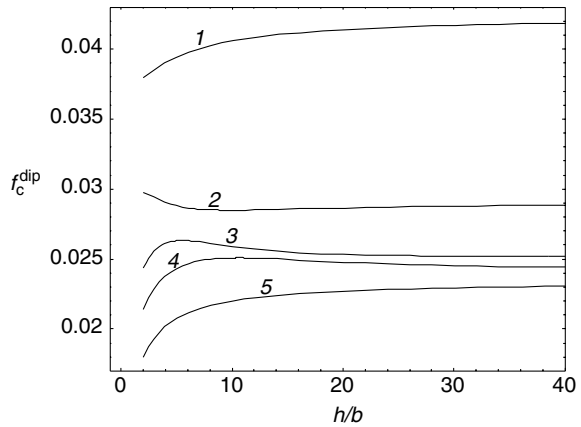

Figure 6. Dependences of the critical misfit parameter f_c^{dip} on the dimensionless interspacing h/b between the nanowire and the matrix free surface, for $\nu = 0.3$, $r_0 = b$, $c/b = 3$; $a/b = 3$, 9, 24, 45 and ∞ (curves 1, 2, 3, 4 and 5, respectively).

critical misfit parameter f_c^{dip} is not essential. Analysis shows that the critical misfit parameter f_c^{dip} decreases with increasing a and/or c at any interspacing h between the nanowire and the composite free surface.

Comparison between figures 3(a) and 6, and between figures 4(c) and 7(a) shows that the critical misfit parameter f_c^{dip} for the formation of dislocation dipoles is lower than the critical misfit parameters f_c^{l} and f_c^{sl} that characterize the energetically favourable formation of dislocation loops and semi-loops, respectively. It should be noted, however, that misfit dislocation dipoles can result from transformations of dislocation semi-loops previously formed in a composite. In these circumstances, real values of the critical misfit parameter f_c^{dip} can exceed those calculated here.

Together with misfit defect configurations (dislocation loops, semi-loops and dipoles) considered in this paper, generally speaking, other defect configurations that cause relaxation of misfit stresses are capable of being formed. In particular, such configurations are dipoles of dislocations located at the nanowire facets $x_2 = \pm a$. Analysis of their formation is the subject of further investigation.

8. Concluding remarks

Here we have suggested a theoretical model which describes the formation of misfit dislocation configurations (loops, semi-loops, dipoles) in composite solids containing nanowires with rectangular sections (figure 1). In the framework of the model, we have theoretically examined the influence of geometric parameters on the formation of these misfit dislocation configurations. The results of our quantitative examinations are in short as follows:

(i) The set of geometric parameters crucially affecting the generation of various misfit dislocation configurations in composites with nanowires contains the misfit parameter f, the nanowire sizes a and c, and the interspacing h between a nanowire and the composite free surface.

(ii) As with the commonly studied situation with plate-like film/substrate composites, the generation of misfit dislocation configurations is energetically favourable in composites with nanowires when their geometric parameters are in certain ranges (calculated above; see figures 2–7).

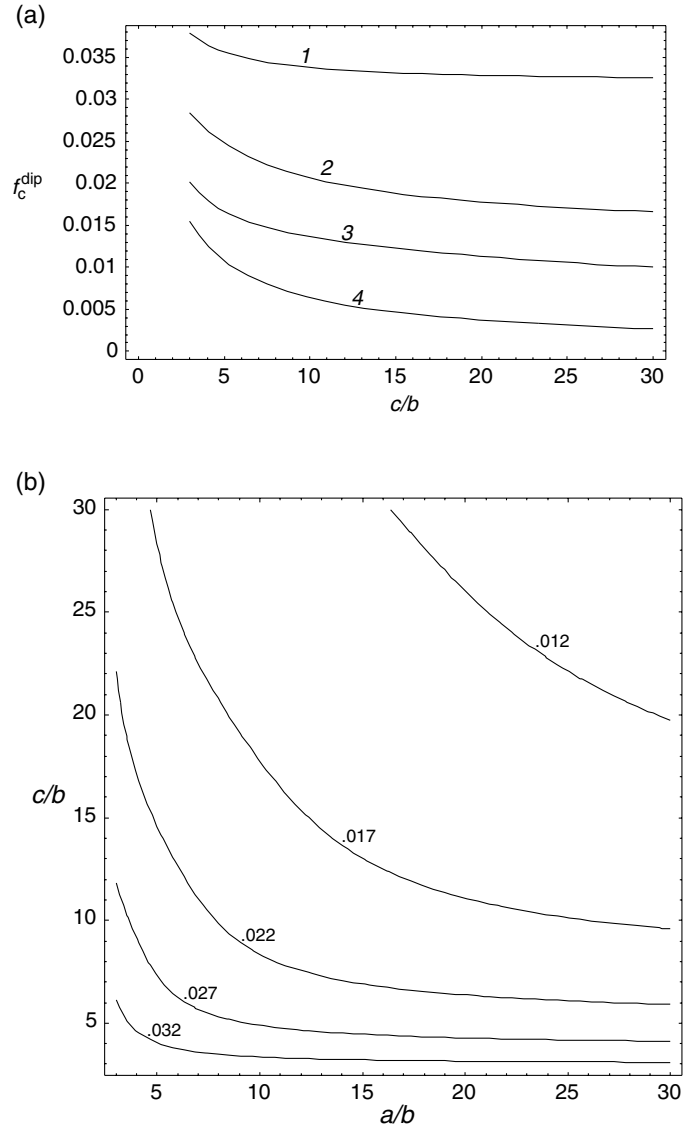

Figure 7. (a) Dependences of the critical misfit parameter f_c^{dip} on the non-dimensional semi-height c/b of the nanowire, for $\nu = 0.3$, $r_0 = h = b$; $a/b = 3$, 10, 30 and ∞ (curves 1, 2, 3 and 4, respectively). (b) The maps of the critical misfit f_c^{dip} in the coordinate space $(a/b, c/b)$ for $\nu = 0.3$, $r_0 = h = b$.

(iii) Different misfit dislocation configurations (loops, semi-loops and dipoles (figure 1)) are energetically preferred in different ranges of geometric parameters, in which case their transformations can occur due to changes in these parameters, say, during deposition of new atomic layers onto the composite free surface.

These results are important for technological applications of nanowires. In most cases the formation of misfit dislocations as recombination centres leads to a dramatic degradation of the functional properties of semiconductor nanowires. Therefore, it is commonly desirable to fabricate nanowires in composites having geometric parameters in ranges corresponding to the

non-defected state. However, the fabrication of a nanowire with misfit defect configurations periodically arranged along the nanowire long axis can serve as a method for synthesis of semiconductor nanowires containing quantum dots, which is an effective alternative to the existing methods [8–10]. Actually, stress field distribution along such a nanowire is capable of causing tentatively periodic modulation of its chemical composition along the nanowire (because atoms of different chemical elements exhibit different behaviours in response to stress fields). It is exactly the case of nanowires with compositionally distinguished quantum dots.

Acknowledgments

This work was supported, in part, by the Office of US Naval Research (grant N00014-01-1-1020), the Office of US Naval Research, International Field Office, Europe (grant N00014-02-1-4045), the Russian Fund of Basic Research (grant 01-02-16853), the Russian State Programme on Solid-State Nanostructures, St Petersburg Scientific Centre of Russian Academy of Sciences, and the 'Integration' Programme (grant B0026).

References

[1] Wegrowe J-E, Sallin A, Fabian A, Comment A, Bonard J-M and Ansermet J-Ph 2002 *Phys. Rev.* B **65** 012407
[2] Zheng M, Menon L, Zeng H, Liu Y, Bandyopadhyay S, Kirby R D and Sellmyer D J 2000 *Phys. Rev.* B **62** 12282–6
[3] Zeng H, Skomski R, Menon L, Liu Y, Bandyopadhyay S and Sellmyer D J 2002 *Phys. Rev.* B **65** 134426
[4] Wang Z K, Kuok M H, Ng S C, Lockwood D J, Cottam M G, Nielsch K, Wehrpohn R B and Gösele U 2002 *Phys. Rev. Lett.* **89** 027201
[5] Heremans J, Trush C M, Lin Y-M, Cronin S B and Dresselhaus M S 2001 *Phys. Rev.* B **63** 085406
[6] Batzill M, Bardou F and Snowdon K J 2001 *Phys. Rev.* B **63** 233408
[7] Rodrigues V, Bettini J, Rocha A R, Rego L G C and Ugarte D 2002 *Phys. Rev.* B **65** 153402
[8] Jorritsma J and Mydosh J A 2000 *Phys. Rev.* B **62** 9703–8
[9] Cui Y and Lieber C M 2001 *Science* **291** 851–3
[10] Gudiksen M S, Lauhon L J, Wang J, Smith D C and Lieber C M 2002 *Nature* **415** 617–20
[11] Priester C and Grenet G 2001 *Phys. Rev.* B **64** 125312
[12] Ovid'ko I A and Sheinerman A G 2001 *J. Phys.: Condens. Matter* **13** 9645–53
[13] Pacifi D, Moreira E C, Franzo G, Martorino V, Priolo F and Iacona F 2002 *Phys. Rev.* B **65** 144109
[14] Sasaki T, Koshizaki N, Koinuma M and Matsumoto Y 1999 *Nanostruct. Mater.* **12** 511–14
[15] He J, Ice M and Lavernia E J 2000 *Nanostructured Films and Coatings (NATO Science Series)* ed G-M Chow, I A Ovid'ko and T Tsakalakos (Dordrecht: Kluwer) pp 131–48
[16] Hwu Y K, Chow G M, Goh W C, Cho T S, Je J H, Noh D Y, Lin H-M and Lin C K 2000 *Nanostructured Films and Coatings (NATO ASI Series)* ed G-M Chow, I A Ovid'ko and T Tsakalakos (Dordrecht: Kluwer) pp 203–14
[17] Vladimirov V I, Gutkin M Yu and Romanov A E 1987 *Sov. Phys.–Solid State* **29** 1581–2
Vladimirov V I, Gutkin M Yu and Romanov A E 1988 *Poverkhn* **6** 46–51
[18] Gutkin M Yu and Romanov A E 1990 *Sov. Phys.–Solid State* **32** 751–3
Gutkin M Yu and Romanov A E 1992 *Phys. Status Solidi* a **129** 117–26
Gutkin M Yu and Romanov A E 1994 *Phys. Status Solidi* a **144** 39–57
[19] Willis J R, Jain S C and Bullough R 1990 *Phil. Mag.* A **62** 115–9
[20] Fitzgerald E A 1991 *Mater. Sci. Rep.* **7** 87–142
[21] van der Merve J H 1991 *Crit. Rev. Solid State Mater. Sci.* **17** 187–209
[22] Atkinson A and Jain S C 1992 *J. Appl. Phys.* **72** 2242–8
[23] Gosling T J, Jain S C, Willis J R, Atkison A and Bullough R 1992 *Phil. Mag.* A **66** 119–32
[24] Gosling T J, Bullough R, Jain S C and Willis J R 1993 *J. Appl. Phys.* **73** 8267–78
[25] Gutkin M Yu, Kolesnikova A L and Romanov A E 1993 *Mater. Sci. Eng.* A **164** 433–7
[26] Gosling T J and Willis J R 1994 *Phil. Mag.* A **69** 65–90
[27] Pehlke E, Moll N, Kley A and Scheffler M 1997 *Appl. Phys.* A **65** 525–34

[28] Johnson H T and Freund L B 1997 *J. Appl. Phys.* **81** 6081–90
[29] Jain S C, Harker A H and Cowley R A 1997 *Phil. Mag.* A **75** 1461–515
[30] Gutkin M Yu, Mikaelyan K N and Ovid'ko I A 1998 *Phys. Solid State* **40** 1864–9
Gutkin M Yu, Mikaelyan K N and Ovid'ko I A 2001 *Phys. Solid State* **43** 82–6
[31] Gutkin M Yu, Ovid'ko I A and Sheinerman A G 2000 *J. Phys.: Condens. Matter* **12** 5391–401
[32] Ovid'ko I A 1999 *J. Phys.: Condens. Matter* **11** 6521–7
Ovid'ko I A 2001 *J. Phys.: Condens. Matter* **13** L97–103
[33] Bobylev S V, Ovid'ko I A and Sheinerman A G 2001 *Phys. Rev.* B **64** 224507
[34] Ovid'ko I A and Sheinerman A G 2001 *J. Phys.: Condens. Matter* **13** 7937–51
[35] Sheinerman A G and Gutkin M Yu 2001 *Phys. Status Solidi* a **184** 485–505
Sheinerman A G and Gutkin M Yu 2001 *Scr. Mater.* **45** 81–7
[36] Ovid'ko I A 2002 *Phys. Rev. Lett.* **88** 046103
[37] Kroupa F 1960 *Czech. J. Phys.* B **10** 284
Kroupa F 1962 *Czech. J. Phys.* B **12** 191
Kroupa F 1962 *Phil. Mag.* **7** 783–801
[38] Baštecká J 1964 *Czech. J. Phys.* B **14** 430–42
[39] Mura T 1968 *Advances in Materials Research* vol 3, ed H Herman (New York: Interscience) pp 1–108
[40] Marchikowsky M S and Sree Harsha K S 1968 *J. Appl. Phys.* **39** 1775–83
[41] Huang W and Mura T 1970 *J. Appl. Phys.* **41** 5175–9
[42] Kolesnikova A L and Romanov A E 1986 *Preprint* No 1019 A F Ioffe Physico-Technical Institute, Leningrad
[43] Khraishi T A, Hirth J P, Zbib H M and Diaz de La Rubia T 2000 *Phil. Mag. Lett.* **80** 95–105
[44] Jäger W, Rühle M and Wilkens M 1975 *Phys. Status Solidi* a **31** 525–33
[45] Ohr S M 1978 *J. Appl. Phys.* **49** 4953–5
[46] Dundurs J and Salamon N J 1972 *Phys. Status Solidi* b **50** 125–33
[47] Salamon N J and Dundurs J 1977 *J. Phys. C: Solid State Phys.* **10** 497–507
[48] Salamon N J and Comninou M 1979 *Phil. Mag.* A **39** 685–91
[49] Chou Y T 1963 *Acta Metall.* **11** 829–34
[50] Chou Y T 1964 *Acta Metall.* **12** 305–10
[51] Sharpe N G *Phil. Mag.* **7** 859–63
[52] Romanov A E and Vladimirov V I 1992 *Dislocations in Solids* vol 9, ed F R N Nabarro (Amsterdam: North-Holland) pp 191–302
[53] Verecký Š, Kratochvíl J and Kroupa F 2002 *Phys. Status Solidi* a **191** 418–26
[54] Khraishi T A and Zbib H M 2002 *Phil. Mag. Lett.* **82** 265–77
[55] Mastrojannis E N, Mura T and Keer L M 1977 *Phil. Mag.* **35** 1137
[56] Dikici M 1993 *Acta Metall.* **41** 879
[57] Dikici M 2001 *Phys. Status Solidi* b **228** 639–49
[58] Mindlin R D 1936 *Proc. 1st Midwest Conf. on Solid Mech.* pp 56–9
[59] Mura T 1987 *Micromechanics of Defects in Solids* (Dordrecht: Martinus Nijhoff)
[60] Tikhonov L V 1967 *Fiz. Met. Metalloved.* **24** 577 (in Russian)
[61] Groves P P and Bacon D J 1970 *Phil. Mag.* **22** 83–91
[62] Bacon D J and Groves P P 1970 *Fundamental Aspects of Dislocation Theory* vol 1, ed J A Simmons, R de Wit and R Bullough (New York: Natl Bur. Stand. (US), spec. publ. 317) pp 35–45
[63] Vagera I 1970 *Czech. J. Phys.* B **20** 702–10
Vagera I 1970 *Czech. J. Phys.* B **20** 1278–84
[64] Hirth J P and Lothe J 1982 *Theory of Dislocations* (New York: Wiley)
[65] Malyshev K L, Gutkin M Yu, Romanov A E, Sitnikova A A and Sorokin L M 1987 *Preprint* No 1109 A F Ioffe Physico-Technical Institute, Leningrad
[66] Gosling T J, Bullough R, Jain S C and Willis J R 1993 *J. Appl. Phys.* **73** 8267–78
[67] Jin Z, Yang S, Mo C and Liu S 1999 *Eur. Phys. J.* **6** 251–5